Modelling the Electrolyte Flow in a Full-scale Copper Electrorefining Tankhouse Cell

Andreas Kemminger, Andreas Ludwig

Montanuniversitaet Leoben
Department Metallurgy, Chair of Simulation and Modelling of Metallurgical Processes
Leoben, Austria

Keywords: Hydrometallurgy, electrolysis, CFD simulation, copper

Abstract

A computational fluid dynamic simulation of the electrolyte flow in a full-scale copper electrorefining tankhouse cell had been performed. The dissolution of copper ions at the impure anodes and their plating onto the cathodes leads to a local density variation along the electrodes and thus to buoyancy-driven flow between anodes and cathodes. Corresponding Cu^{++} concentration fields together with the resulting natural convection pattern were simulated by means of a "local" simulation. As the predicted concentration and velocity fields within the gaps were mainly independent of global flow phenomena, representative results were used as inlet information for 120 interfaces that link the "local" simulation to a "global" simulation. With such a hybrid-approach it was possible to simulate both small-scale flow phenomena between the electrodes and large-scale flow phenomena in the full-scale industrial tankhouse cell. The results suggest that fresh electrolyte is first pushed down by the flow leaving the electrode gaps, and then guided to the side of the tankhouse cell from where it is sucked into the upper part of the electrode gaps.

1 Introduction

The copper refining electrolysis process is essential to produce high purity copper at industrial scale. High purity copper is needed in electrical applications like conductors, where a high electric conductivity is necessary [1]. The fundamental steps of copper refining are:

1. electrochemical dissolving copper from impure anodes into a $CuSO_4$-H_2SO_4-H_2O electrolyte;
2. electrochemical plating pure copper (without the anode impurities) from the electrolyte onto stainless steel copper cathodes.

The main purpose is not only to produce pure copper that is essentially free of harmful impurities but also to separate valuable impurities (e. g. gold and silver) from the anodic copper for later recovery [2].

2 Numerical model

A numerical calculation of fluid flow or heat flow is only possible if the physical laws can be transformed into mathematical equations, normally into differential equations. Each single differential equation is linked to a certain conservation law and consists of one physical value as a depended variable. It is assumed that the different factors influencing the physical value are in equilibrium. The dependent variable of these differential equations are used as specific value, which means that it is calculated for one control volume. Examples are the velocity (momentum per control volume), mass and specific enthalpy/energy [3].

With the continuity equation (1) and the momentum conservation equation (2) the flow of the electrolyte and with the species conservation equation (3) the variation in Cu^{++} cations concentration was calculated.

$$\frac{\partial \rho}{\partial t} + \nabla \cdot (\rho \vec{v}) = 0 \tag{1}$$

$$\frac{\partial}{\partial t}(\rho \vec{v}) + \nabla \cdot (\rho \vec{v} \vec{v}) = \nabla p + \nabla \cdot (\bar{\bar{\tau}}) + \rho \vec{g} + \vec{F} \tag{2}$$

$$\frac{\partial}{\partial t}(\rho c) + \nabla \cdot (\rho \vec{v} c) + \nabla \cdot (-D \nabla c) = \dot{Q}_c \tag{3}$$

In the formula ρ is the density of the electrolyte, p the static pressure, $\bar{\bar{\tau}}$ the stress tensor and $\rho \vec{g}$ and $\vec{F}$ are the gravitational body force and external body forces that arise from dissolving and plating of copper as used by Leahy [4]. The external body force given by equation (4) represents a boussinesq approximation [5]. By using this approach the density ρ can be considered constant in the conservation equations (1) and (2). D is the diffusion coefficient. The quantity $\dot{Q}_c$ represents the rate of dissolution and plating of the Cu^{++} cations. The dissolution happens at the anode where the copper cations enter the numerical domain. Cations are transported to the cathode by diffusion and convection where they are plated i.e. taken out of the numerical domain. Therefore, $\dot{Q}_c$ has a positive value on the anode and a negative value at the cathode. In the rest of the numerical domain it is set to zero. As shown in equation (5), $\dot{Q}_c$ is governed by the current density j.

$$\vec{F} = -\rho \cdot \vec{g} \cdot \beta \cdot (c - c_0) \tag{4}$$

$$\dot{Q}_c = \begin{cases} \pm \dfrac{j \cdot m_{Cu}}{z \cdot F_a} & \text{with (+) on cathode and (-) on anode} \\ 0 & \text{elsewhere} \end{cases} \tag{5}$$

The current density is calculated only at the surface of every cathode and anode by using the Butler-Volmer equation [6] as shown in equation (6).

$$j = j_a \cdot \exp\left(\frac{\alpha_a \cdot z \cdot F_a \cdot \mu_a}{R \cdot T}\right) - j_c \cdot \left(\frac{c}{c_0}\right) \cdot \exp\left(\frac{\alpha_c \cdot z \cdot F_a \cdot \mu_c}{R \cdot T}\right) \quad (6)$$

The equations are closed with a set of model parameters, given in Table 1. The CFD model is set up within the ANSYS Fluent 14.5 framework [7].

Table 1: Model parameters

Parameter		Value	Unit
ρ	density	1220	kg m^{-3}
c_0	initial Copper concentration	45.5	kg m^{-3}
β	solutal expansion coefficient	$2.2 \cdot 10^{-3}$	m³ kg^{-1}
D	diffusion coefficient	$1.125 \cdot 10^{-6}$	kg m^{-1} s^{-1}
m_{Cu}	molar mass of Cu	0.064	kg mol^{-1}
z	Current number (No. of electrons per Cu^{++} cation)	2	-
F_a	Faraday constant	96485	C mol^{-1}
α_a, α_c	anodic, cathodic transfer coefficient	0.6, 0.4	-
μ_a, μ_c	anodic; cathodic overpotential	0.01, 0.08	V
T	electrolyte temperature	338.15	K
j_a, j_c	anodic, cathodic exchange current	258	A m^{-2}

3 Simulation strategy and problem description

The simulation of copper electrolysis has been the topic of a number of research papers. While most frequently the natural convection is simulated in small-scale test domains ([6], [8], [9] and [10]) or in large-scale 2D domains ([11] and [12]), this paper tackles the simulation of the flow pattern caused by the interaction of natural and forced convection in a full-scale copper electrorefining tankhouse cell.

Industrial tankhouse cells can reach an overall length of several meters. They usually consist of up to 60 cathodes and 61 anodes. Since the natural convection is based on a concentration variation in the vicinity of the electrodes, the numerical grid must be very fine in these areas in order to achieve a sufficient accurate solution. On the other hand, the large size of an industrial electrolysis tankhouse cell (see Figure 1) would make more than a billion numerical volume elements necessary and thus, considering the today's computer technology, a simultaneous calculation of natural and forced

convection in a full-scale simulation domain is unpractical, if not impossible. Therefore, the simulation had to be separated into two steps. First, the flow of the electrolyte caused by natural convection in a typical anode-cathode gap was simulated with a so-called "local" simulation. Here, a very fine meshing of the numeric grid at the anode and cathode was applied in order to get a sufficient resolution of the solutal and momentum boundary layers (see Figure 2). The simulation of the forced convection is then done as so-called "global" simulation, where the simulation domain consisted of the whole tankhouse cell apart from the gaps between anodes and cathodes. These were blocked off in order to keep the size of the numeric grid at a maintainable level. The link between the local simulation of natural convection between the electrodes and the global simulation of the force convection in the full-scale tankhouse cell was done by introducing a series of interfaces allowing the transfer of velocity- and concentration profiles from the local to the global simulation (see Figure 3).

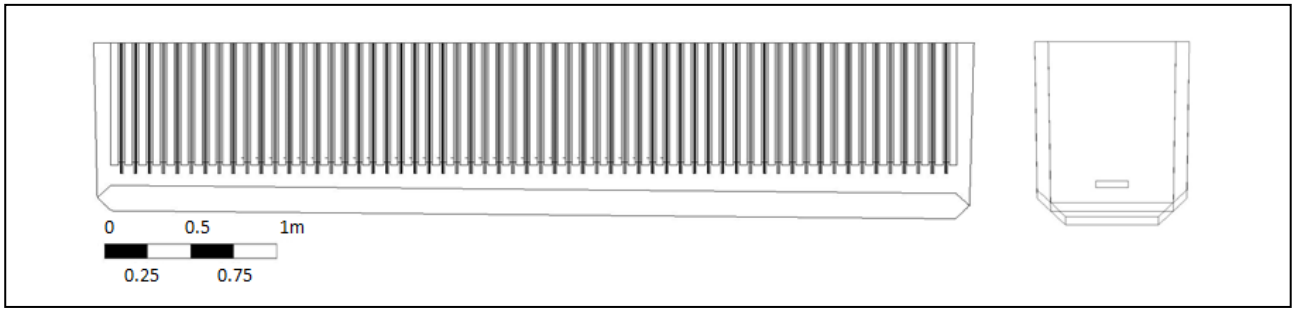

Figure 1: Geometry of an industrial used tankhouse cell with the alternating assembly of anodes and cathodes.

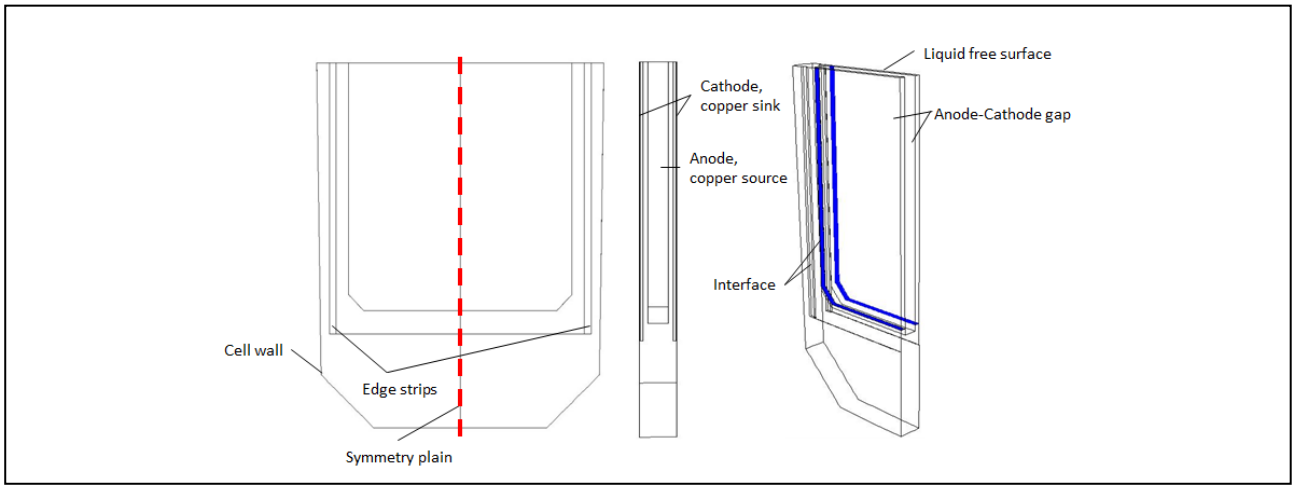

Figure 2: The local simulation domain covered the area between two cathodes. Because of the symmetry only half of the domain was modelled. A very fine mesh was used in order to get an adequate solution of concentration- and velocity gradients at the electrodes. The velocity- and copper profiles at the interfaces defined to link local and global simulation are later used as inlet information for the global simulation.

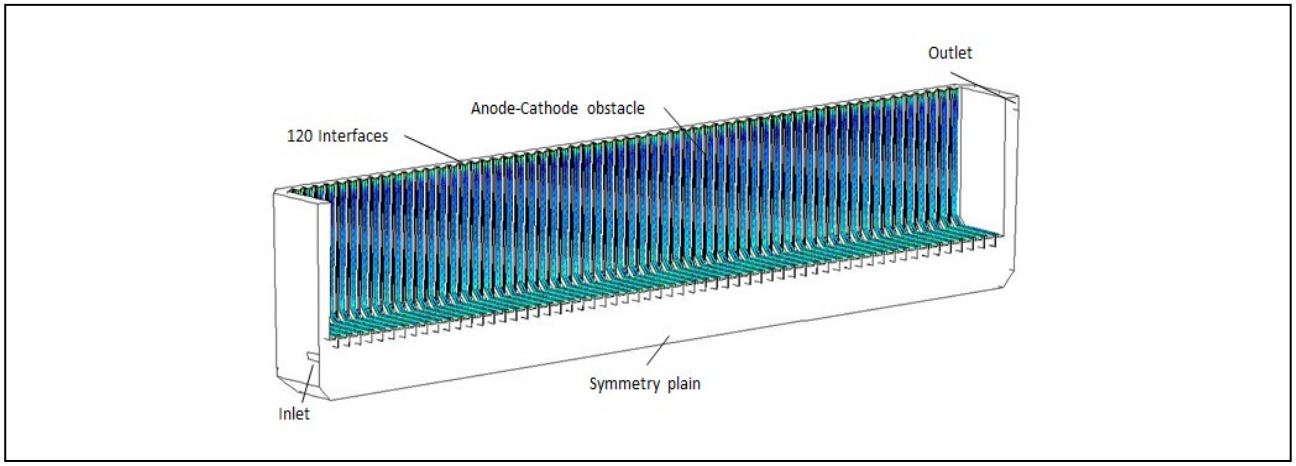

Figure 3: The global simulation domain covered the whole tankhouse cell except for the gaps between anodes and cathodes. Here, interfaces were defined with which the dynamic of the natural convection occurring between the electrodes were transferred from the local to the global simulation.

4 Simulation results

4.1 Local simulation

In order to study the natural convection occurring along the electrodes a so-called local simulation of the Cu^{++} concentration and the 3D velocity field between the electrodes were done. The local simulation domain included one anode and two cathodes (with the attached edge strips). The geometry for the detailed cathode-cathode simulation is shown in Figure 2. To achieve a better solution of the concentration and velocity boundary layers the size of the volume elements at the electrodes was set to 500 µm. To decrease the total number of volume elements in the domain and therefore decrease the computation time, only half of the symmetric anode-cathode pair was simulated. A transient simulation was performed until a steady-state velocity profile at the interfaces mentioned in the last section were found.

The boundary conditions for the flux of copper at the anode and cathode was based on the Faraday law as given by equation (5). A positive flux is applied on the anode and a negative flux on the cathode. At the walls no slip boundary conditions are applied while on the “free” top surface a no friction boundary condition was applied.

The electrochemical reactions cause the dissolution of Cu^{++} cations at the anode and their deposition at the cathode. Therefore, a gradient of concentration forms between the electrodes. Figure 4 shows a detailed view of the Cu^{++} concentration in the anode-cathode gap at different heights.

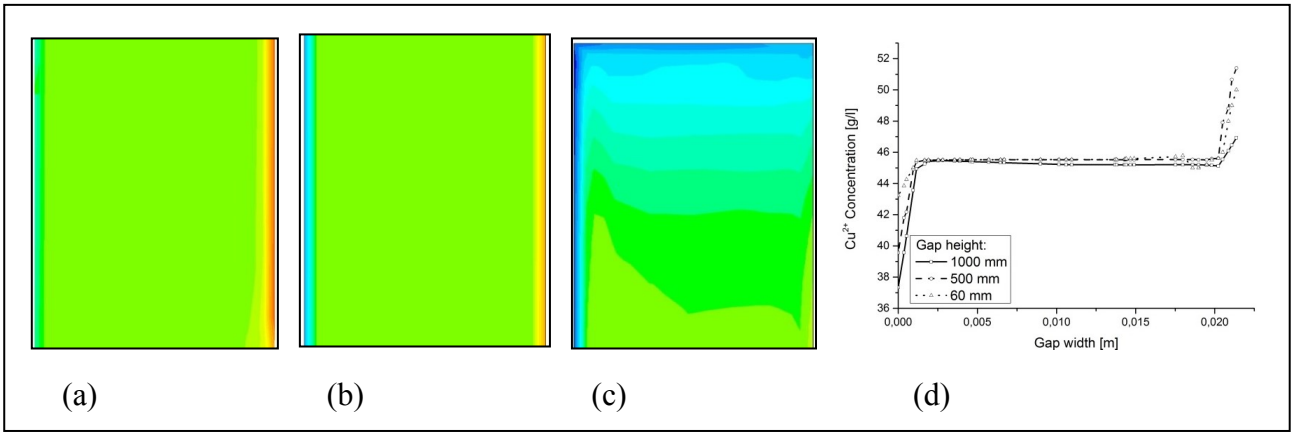

Figure 4: Concentration distribution in the gap between cathode (left) and anode (right) (a) 60 mm above the lower end of the anode, (b) 500 mm, (c) 1000 mm and (d) diagram plot of Cu^{++} concentration profile across the gap. Note that (a), (b) and (c) had to be scaled by a factor of 4 to better visualize the concentration distribution.

This concentration gradient leads to a convective electrolyte flux as shown in Figure 5. The low density in front of the cathode causes an upward movement while the higher density at the anode leads to a downward movement of the electrolyte. The velocity of the electrolyte changes with height. At the top of the anode only a small amount of Cu^{++} has been added to the electrolyte already and the downward movement is very slow. While moving downward along the anode more Cu^{++} is added to the electrolyte causing a stronger buoyancy force and a faster movement. Therefore, the highest downward velocity can be found at the bottom of the anode where also the concentration of Cu^{++} reaches its highest numbers. At the cathode the opposite mechanism happens.

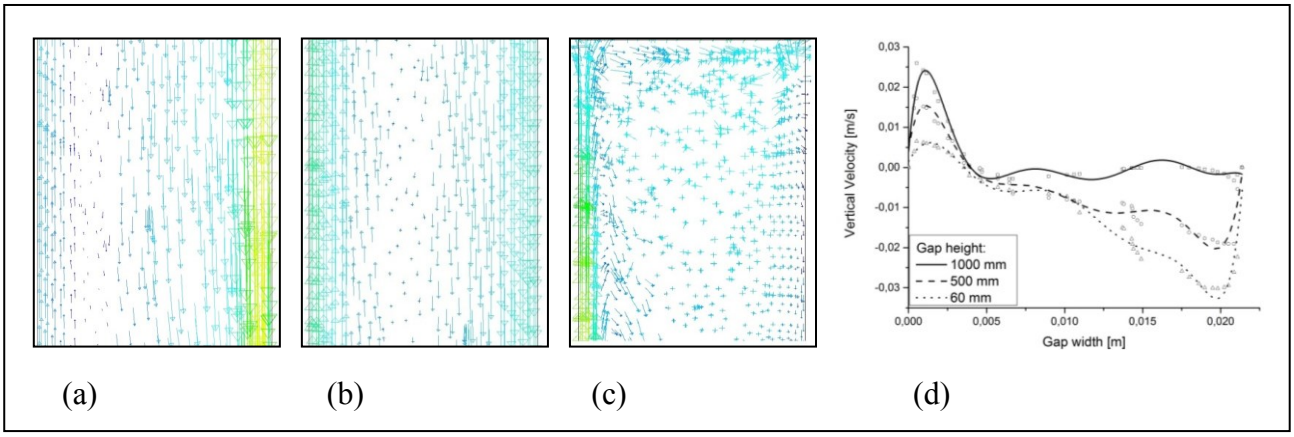

Figure 5: Velocity vectors in the gap (a) 60 mm above the lower end of the anode, (b) 500 mm, (c) 1000 mm and (d) diagram plot of vertical velocity over the gap width. Note that (a), (b) and (c) had to be scaled by a factor of 4 to better visualize the results.

Figure 6 shows the copper concentration directly in front of the anode and cathode. Clearly visible is the stacking of layers with different concentrations. The downward movement of electrolyte at

the anode transports the cations to the lower part of the anode. While moving, more and more cations are loaded into the electrolyte resulting in a high concentration at the bottom part of the anode. The opposite can be seen at the cathode. While moving upward, more cations are removed from the electrolyte leading to a low concentration of Cu^{++} at the top.

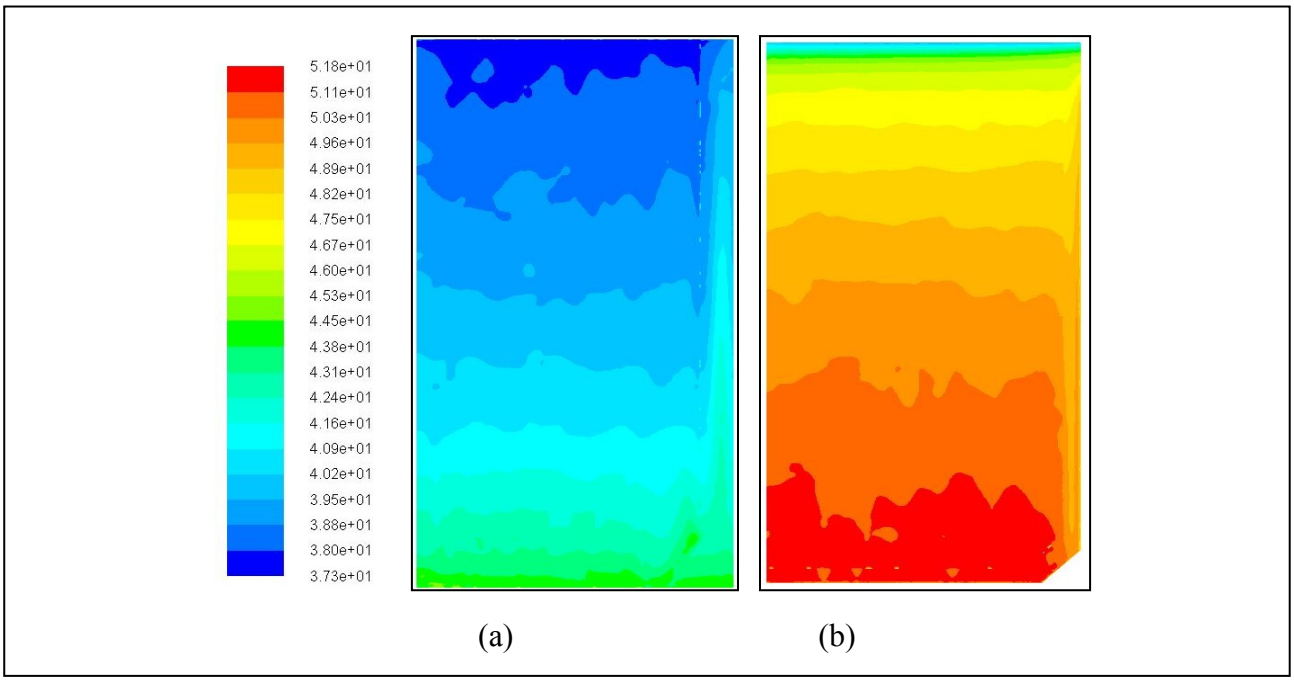

Figure 6: Cu^{++} concentration in kg m^{-3} adjacent to the cathode (a), and adjacent to the anode (b).

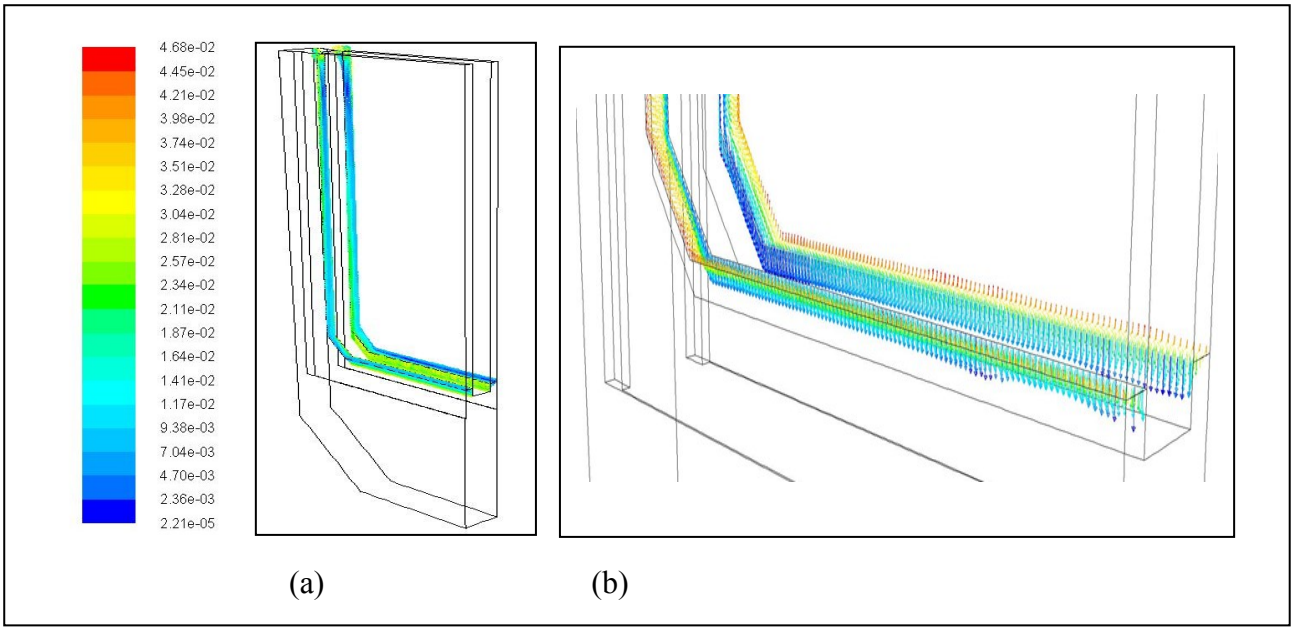

Figure 7: Velocity profile at the interface linking local and global simulations in m s^{-1} (a) the integral of the mass flow equals zero and thus the mass is conserved along the interface, (b) Detailed view of the interface at the bottom; the downward movement along the anode is stronger than the upward movement at the cathode.

We have performed several local simulations by assuming different in- and outlet conditions at the front and back faces of the domain. It turned out that the flow between the electrodes was only little influenced by the in- and outlet conditions, especially for the flow at some distance from the edges of the electrodes. Thus, the flow field at the interface linking local and global simulations, shown in Figure 7, seems to be a universal one, which mainly depends on the phenomena happening between the anode and cathode, and which is marginally affected by the global flow. Although it seems that the downward movement at the anode dominates the flow, the total mass crossing the interface is zero. Velocity profiles as the ones shown in Figure 7 were taken as inlet profiles for the global simulations at the 120 interfaces linking local and global simulations.

4.2 Global Simulation

With the global simulation the flow field in the whole tankhouse cell governed by both force convection via an in- and outlet and natural convection via the 120 “gap” inlets were estimated. As mentioned above, the velocity profiles gained from the local simulation were used at these inlets. The corresponding interfaces linking global and local simulations were located 50 mm above the lower end of the anodes. This position was chosen because numerous simulation trials showed that the flow between the electrodes were negligibly affected by any global flow details. Therefore, the assumed one-way coupling between the local and global simulation is justified and the same velocity profiles can be used for all anode-cathode “gap” inlets.

Figure 8 shows the input values for the “gap” interfaces gained by the local simulation. The forced convection caused by the pumping of fresh electrolyte in and out of the tankhouse cell forms a free jet at the inlet. This free jet interacts with the natural convection from between the anode-cathode gaps and is thus pushed down, see Figure 8b) and 9. The flow patterns underneath the electrodes are shown in Figure 10 in details. It can be seen that the electrolyte flows from the bottom to the side of the tankhouse cell, where it moves up and is then drawn into the upper part of the gap between the electrodes.

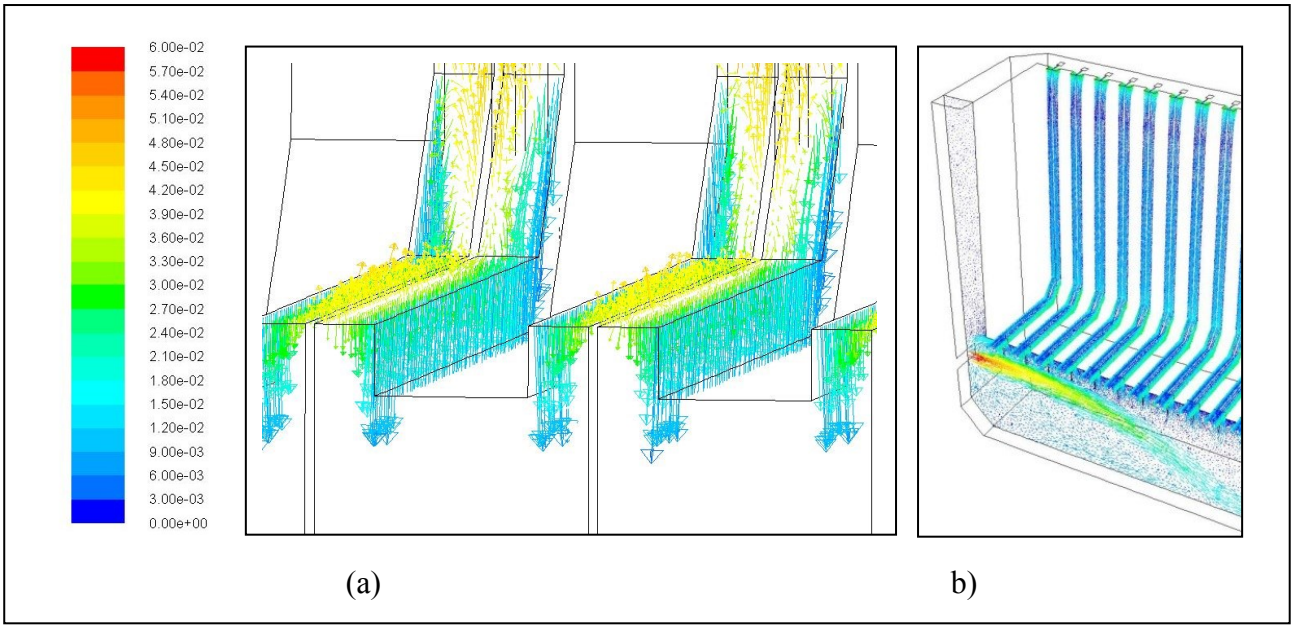

Figure 8: (a) Velocity profile gained from the local simulation and used as boundary conditions for the global simulation at the 120 "gap" interfaces, and (b) the fresh electrolyte jet stream from the inlet of the tankhouse cell interacts with the natural convection from the anode-cathode gaps (velocity vectors in m s^{-1}).

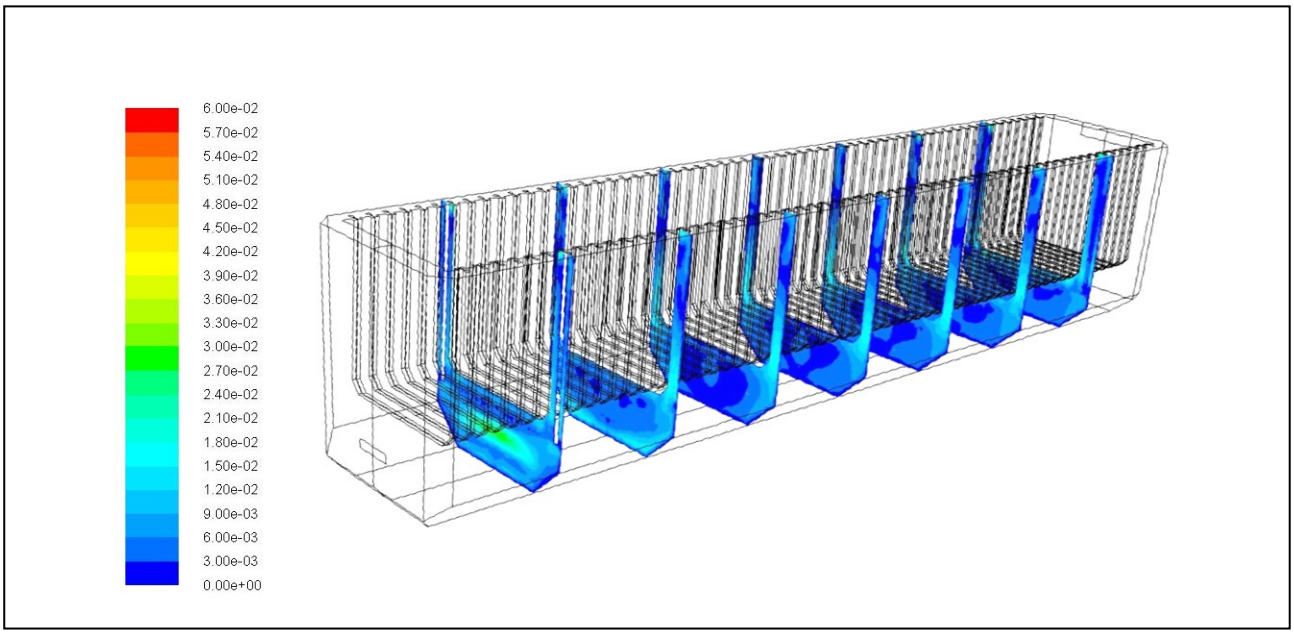

Figure 9: Contour plots (in m s^{-1}) of the global flow field plotted on different planes in the tankhouse cell. High velocities can be found in the bulk area underneath the electrodes close to the inlet as well as between the electrodes and the outer walls.

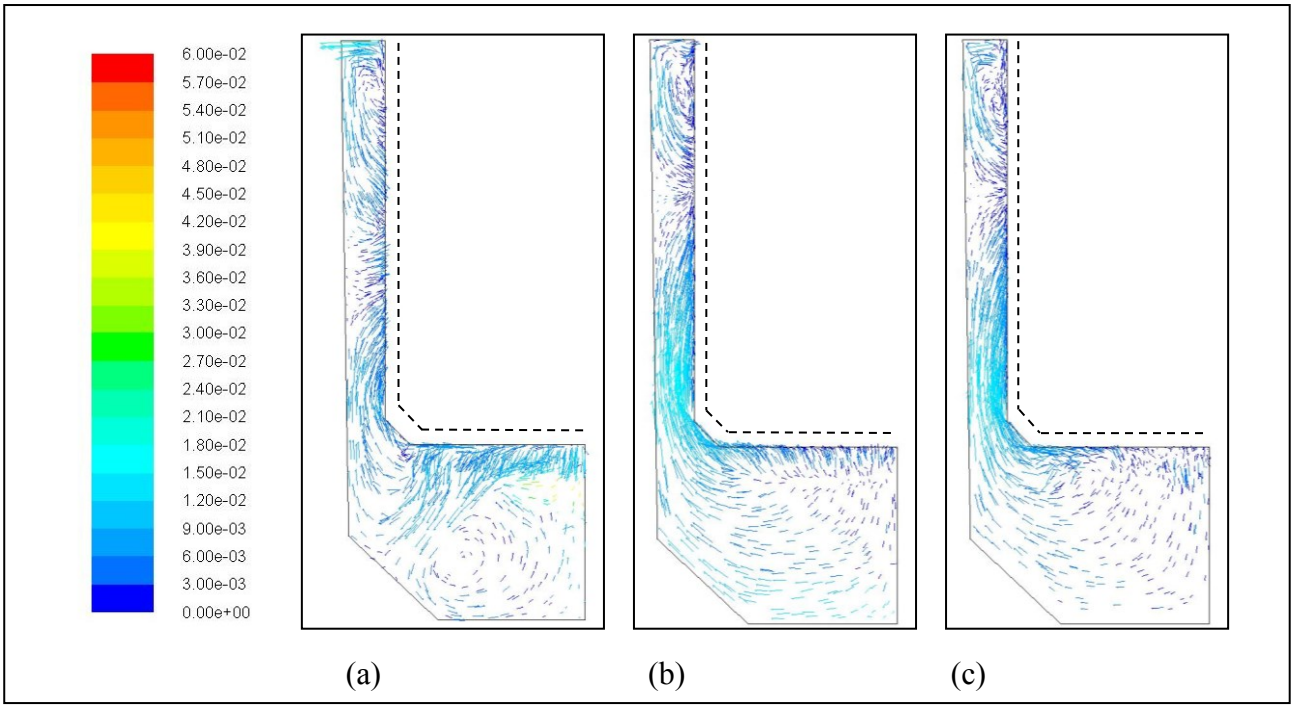

Figure 10: Velocity vectors (in m s^{-1}) at three planes in the tankhouse cell (a) at the first anode-cathode gap, (b) at the 5th anode-cathode gap, (c) at the 10th anode-cathode gap. The dotted line shows the position of the interface used to link local and global simulations. Besides to some disturbances at the first gap, the electrolyte moves from the bottom of the electrodes to the sides, where it is drawn into the upper part of the gap between the electrodes.

5 Conclusion

The presented simulation approach enables the CFD simulation of a full scale copper electrorefining tankhouse cell including the natural convection in between two representative anode-cathode gaps. The density changes that are responsible for the occurring convective electrolyte movement are taking place just in front of the anode and cathode surfaces. Due to the size difference between corresponding boundary layers and the dimensions of industrial copper electrorefining tankhouse cells, a direct numerical simulation combining natural and forced convection in one singe simulation is principally conceivable but because of available hardware power still impossible. These limitations can be overcome by separating the simulation into two distinctive steps. First, the electrolyte flow caused by natural convection in the gap between the electrodes can be modelled with a “local” simulation using a very fine numerical grid. In a second step a “global” simulation can be applied to simulate the interaction of natural and forced convection in the full-scale industrial tankhouse cell.

The present results show that (i) the flow in the gap between the electrode is mainly governed by natural convection caused by density changes of the electrolyte, and (ii) the inlet jet into the full-

scale tankhouse cell is pushed downwards by the flow from the array of electrode gaps and then guided to the tankhouse cell sides from where it is drawn into the electrode gaps. The last finding suggests that fresh inhibitor generally enters the electrode gaps from upper side areas. Further studies including experimental verifications are required to understand the influence of fresh electrolyte intake on the distribution of these surface active agents in more details.

References

[1] DAVENPORT W.G., M. KING, M. SCHLESINGER AND A.K. BISWAS, Extractive Metallurgy of Copper, 4th edition, Pergamon publishing (2002), 265.

[2] PAWLEK F., Metallhüttenkunde, Walter de Gruyter, Berlin - New York, (1983), 601-611.

[3] PATANKAR S.V, Numerical Heat Transfer and Fluid Flow, Series in Computational Methods in Mechanics and Thermal Sciences, Hemisphere Publishing Corporation, (1980), 11-23.

[4] LEAHY M.J. & P. SCHWARTZ, Experimental validation of a computational fluid dynamics model of copper electrowinning, Metallurgical and Materials Transactions B 41, (2010) No. 6, 1247-1260.

[5] PLAWSKY J., Transport Phenomena Fundamentals, 2nd Edition, CRC Press Taylor and Francis Group, (2010), 203-208.

[6] DOCHE O., F. BAUER & S. TARDU, Direct simulation of an electrolyte deposition under a turbulent flow – A first approach, Journal of Electrochemical Chemistry 664 (2012), 1-6.

[7] ANSYS, FLUENT 14.5, ANSYS Inc., Canonsburg, USA, (2012), website www.ansys.com/cfx.

[8] KONISHI Y., Y. TANAKA, Y. KONDO & Y. FUKUNAKA, Copper dissolution phenomena along vertical plane anode in CuSO4 solution, Electrochemica Acta 46 (2000), 681-690.

[9] KAWAI S., K. NISHIKAWA, Y. FUKUNAKA, S. KIDA, Numerical simulation of transient natural convection induced by electrochemical reactions confined between vertical plane Cu electrodes, Electrochemica Acta 53 (2007), 257-264.

[10] XUEGENG Y., K. ECKERT, K. SEIDEL & M. UHLEMANN, The startup of natural convection during copper electrolysis in the presence of an opposing Lorentz force, Electrochemica Acta 54 (2008), 352-359.

[11] LEAHY, M.J. & P. SCHWARZ, Modelling natural convection in copper electrorefining: Describing turbulence behaviour for industrial-sized-systems, Metallurgical and Materials Transaction B 42 (2011), 875-890.

[12] FILZWIESER, A., A. LACKNER & K. HEIN, Möglichkeiten zur Strömungsberechnng in Elektrolysezellen unter besonderer Berücksichtigung des Stofftransportes, Heft 81 der Schriftreihe der GDMB (1998), 161-172.